J|A|C|S COMMUNICATIONS

Published on Web 01/12/2010

Electrochemical Proton-Coupled Electron Transfer of an Osmium Aquo Complex: Theoretical Analysis of Asymmetric Tafel Plots and Transfer Coefficients

Michelle K. Ludlow, Alexander V. Soudackov, and Sharon Hammes-Schiffer*

Department of Chemistry, 104 Chemistry Building, Pennsylvania State University, University Park, Pennsylvania 16802

Received December 4, 2009; E-mail: shs@chem.psu.edu

Electrochemical proton-coupled electron transfer (PCET) at metal−solution interfaces is significant in a broad range of energy devices, including photovoltaics and solar fuel cells. Although homogeneous PCET reactions have been studied extensively,[1−6] electrochemical PCET reactions have only recently started to attract widespread interest.[6−8] A notable example is PCET of an osmium aquo complex attached to a self-assembled monolayer (SAM) on a gold electrode, as depicted in Figure 1. Analysis of the cyclic voltammetry data for this process indicates that this reaction occurs by a concerted PCET mechanism,[9,10] as supported by a hydrogen/deuterium kinetic isotope effect (KIE) of approximately 2 for pH > 4.[9] Kinetic analysis of the reaction pathways suggests that water and OH^- are not viable proton acceptors and that the terminal carboxylate (CO_2^-) groups on the long-chain thiols in the SAM are probable proton acceptors.[10] The p$K_a \approx 5$ of the terminal COOH groups is consistent with the appearance of the KIE at pH > 4. The Tafel plots are asymmetric, and the cathodic transfer coefficient at zero overpotential, $\alpha_{PCET}(0)$, deviates from the standard value of one-half.[9]

This Communication provides a physical explanation for the asymmetric Tafel plots and the deviation of $\alpha_{PCET}(0)$ from one-half, as well as experimentally testable predictions of how specific system properties impact these experimental observables. Previously, these experimental results were explained in terms of different reorganization energies for the cathodic and anodic processes. This previous analysis was based on rate constant expressions assuming a fixed proton donor−acceptor distance. In the present work, we include the effects of changes in the equilibrium proton donor−acceptor distance upon oxidation or reduction,[11] leading to an alternative explanation for the asymmetric Tafel plots and deviation of $\alpha_{PCET}(0)$ from one-half.

Our analysis is based on the following approximate expressions for the heterogeneous PCET anodic and cathodic nonadiabatic rate constants:[8]

$$k_a(\eta) = \frac{(V^{el}S)^2}{\hbar}\sqrt{\frac{\pi}{k_B T\Lambda}}\exp[2\alpha^2 k_B T/F_R]\rho_M \times \int d\varepsilon[1 - f(\varepsilon)]\exp\left[-\frac{(\Delta\tilde{U} + \varepsilon - e\eta + \Lambda + 2\alpha\delta R k_B T)^2}{4\Lambda k_B T}\right]$$

$$k_c(\eta) = \frac{(V^{el}S)^2}{\hbar}\sqrt{\frac{\pi}{k_B T\Lambda}}\exp[-2\alpha\delta R + 2\alpha^2 k_B T/F_R]\rho_M \times \int d\varepsilon f(\varepsilon)\exp\left[-\frac{(-\Delta\tilde{U} - \varepsilon + e\eta + \Lambda - 2\alpha\delta R k_B T)^2}{4\Lambda k_B T}\right] \quad (1)$$

Here $f(\varepsilon)$ is the Fermi distribution function for the electronic states in the electrode, ρ_M is the density of states at the Fermi level, η is the overpotential defined as the difference between the applied and formal electrode potentials, V^{el} is the electronic coupling, δR is the difference between the equilibrium proton donor−acceptor distances for the oxidized and reduced complexes, F_R is the force constant associated with the proton donor−acceptor mode, S is the overlap integral between the ground reactant and product proton vibrational wave functions, $\alpha = -\partial \ln S/\partial R$, and $\Lambda = \lambda_s + \lambda_R$ is the total reorganization energy, where λ_s is the solvent reorganization energy and $\lambda_R = F_R\,\delta R^2/2$ is the reorganization energy of the proton donor−acceptor mode. The associated cathodic transfer coefficient at small overpotential η is[8]

$$\alpha_{PCET}(\eta) = \frac{1}{2} - \frac{\alpha\delta R k_B T}{\Lambda} + \frac{e\eta}{2\Lambda} \quad (2)$$

The $\pm 2\alpha\delta R k_B T$ terms in the exponentials of eqs 1 lead to asymmetry of the Tafel plots, and the $\alpha\delta R k_B T/\Lambda$ term in eq 2 leads to deviation of $\alpha_{PCET}(0)$ from one-half.

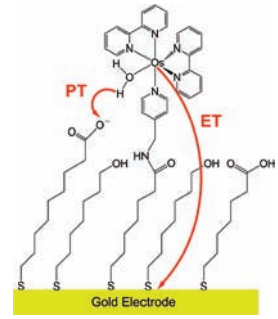

Figure 1. Schematic depiction of the osmium complex attached to a mixed SAM on a gold electrode.

We determined the input quantities for the rate constants by performing density functional theory (DFT) calculations on model systems with Gaussian03.[12] We optimized the gas phase geometries for the osmium complex comprised of $[Os(bpy)_2(4\text{-aminomethylpyridine})(H_2O)]^{2+/3+}$ hydrogen bonded to $CH_3CH_2COO^-$ in both the reduced and oxidized forms at the B3LYP/LANL2DZ level. The calculated proton donor−acceptor O−O distances are 2.49 Å and 2.66 Å for the reduced and oxidized complexes, respectively, leading to $\delta R = 0.17$ Å, and the proton donor−acceptor mode reorganization energy is calculated to be $\lambda_R = 1.62$ kcal/mol from the force constant for the normal mode with the dominant contribution to the O−O vibrational motion. The solvent reorganization energy was calculated to be $\lambda_s = 15.7$ kcal/mol using a dielectric continuum model[13] that depends on the cavity radius of the solute complex, estimated to be 4.87 Å from the optimized reduced osmium complex, the thickness of the SAM, estimated to be 20.64 Å from a DFT B3LYP/6-31G** optimization of $HS(CH_2)_{15}COOH$, and the static and optical dielectric constants of the solvent, SAM, and electrode.

10.1021/ja910277p

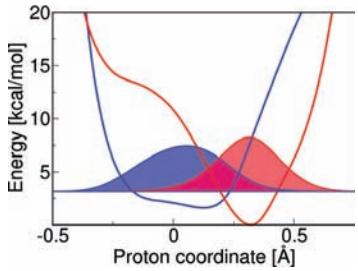

Figure 2. Solvated proton potential energy curves and associated ground state hydrogen vibrational wave functions for the reduced (blue) and oxidized (red) osmium complex hydrogen bonded to a carboxylate group. The potentials are shifted so the ground vibrational states are degenerate.

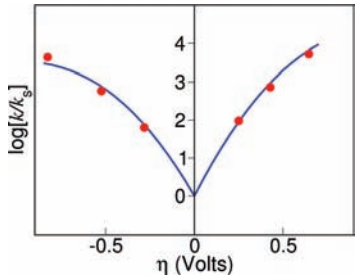

Figure 3. Tafel plot of $\log[k_c/k_s]$ for $\eta < 0$ and $\log[k_o/k_s]$ for $\eta > 0$ calculated using eqs 1 (blue line). The experimental data generated at pH 6.0 obtained from Figure 6 in ref 9 are shown as red filled circles.

The proton potentials were generated on a grid for both the reduced and oxidized osmium complexes by constraining the OH distance while optimizing the two associated angles and the other H atom on the water, followed by single-point energy calculations using the polarized continuum model to include solvation effects. The proton potentials and the associated proton vibrational wave functions[14] are depicted in Figure 2. Note that the carboxylate ion from the SAM may not have the flexibility to adopt the equilibrium geometry obtained from the DFT calculations, thereby impacting the proton potentials and interface parameters. Although the quantitative values of the rates and KIEs are influenced by these aspects, the qualitative trends are reproduced and elucidated by these model calculations.

Figure 3 depicts the calculated anodic and cathodic heterogeneous rate constants as a function of overpotential. No parameters were fit to the experimental data. The prefactors in eqs 1 cancel out because these rate constants are scaled by the standard rate constant k_s (i.e., the rate constants at zero overpotential). The calculated rate constants are in excellent agreement with the experimental data. Equations 1 include only the ground vibronic states, but inclusion of excited vibronic states with fixed α does not alter the qualitative results. The cathodic transfer coefficient was calculated to be $\alpha_{PCET}(0) = 0.47$, which is in agreement with the experimental value of $\alpha_{PCET}(0) = 0.46 \pm 0.02$ reported in ref 9.

The calculated KIE for the standard rate constant is 2.0, which is consistent with the experimental value of $\sim$2. As shown in Figure 2, the ground state proton vibrational wave function for the reduced osmium complex is delocalized between the proton donor and acceptor, leading to a relatively large overlap between the ground state wave functions. In this case, the overlaps corresponding to excited proton vibrational states are significantly smaller due to oscillations of the wave functions, so the ground vibronic states are dominant in the overall rate constant. The relatively large overlap for the dominant pair of vibronic states provides an explanation for the moderate KIE.[6]

The proton acceptor has been hypothesized to be a water molecule, a hydroxide ion, or a carboxylate ion from the SAM. Since the experimental measurements were performed at relatively low pH values, the concentration of hydroxide ions is not expected to be high enough for the hydroxide ion to be the proton acceptor. We considered the possibility of water as the proton acceptor and performed analogous calculations as those described above with water instead of carboxylate as the proton acceptor. For the case of water as the proton acceptor, however, the solvated proton potential energy curves for both the reduced and oxidized forms of the osmium complex have a minimum localized near the water ligated to the osmium (i.e., the proton donor). Moreover, in this case, δR is negative (i.e., the equilibrium proton donor−acceptor distance decreases upon oxidation), which would lead to the opposite asymmetry in the Tafel plot and a cathodic transfer coefficient greater than one-half at zero overpotential. These results are inconsistent with the experimental data, implying that water is not the proton acceptor.

In this theoretical framework, the asymmetry of the Tafel plot and the deviation of the transfer coefficient at zero overpotential from one-half arise from the change in the equilibrium proton donor−acceptor distance upon electron transfer. According to this theory, the direction of the asymmetry and deviation from one-half is determined by the sign of this distance change, and the magnitude of these effects is determined by the magnitude of this distance change, as well as the reorganization energy and the distance dependence of the overlap between the initial and final proton vibrational wave functions. Thus, this theory provides experimentally testable predictions for the impact of specific system properties on the qualitative behavior of the Tafel plots.

Acknowledgment. We acknowledge financial support from NSF Grant No. CHE-07-49646.

Supporting Information Available: Details of heterogeneous rate constants; optimized structures and energies for reduced and oxidized osmium complexes and $HS(CH_2)_{15}COOH$; details of solvent reorganization energy and proton potentials; gas phase and solvated proton potential energy curves with carboxylate as acceptor; solvated proton potential energy curves with water as acceptor; rate constants including excited vibronic states; sensitivity analysis of the Tafel plot with respect to parameter values; complete ref 12. This material is available free of charge via the Internet at http://pubs.acs.org.

References

(1) Cukier, R. I.; Nocera, D. G. *Annu. Rev. Phys. Chem.* **1998**, *49*, 337–369.
(2) Hammes-Schiffer, S. *Acc. Chem. Res.* **2001**, *34*, 273–281.
(3) Mayer, J. M. *Annu. Rev. Phys. Chem.* **2004**, *55*, 363–390.
(4) Huynh, M. H.; Meyer, T. J. *Chem. Rev.* **2007**, *107*, 5004–5064.
(5) Irebo, T.; Reece, S. Y.; Sjödin, M.; Nocera, D. G.; Hammarström, L. *J. Am. Chem. Soc.* **2007**, *129*, 15462–15463.
(6) Hammes-Schiffer, S.; Soudackov, A. V. *J. Phys. Chem. B* **2008**, *112*, 14108–14123.
(7) Costentin, C.; Robert, M.; Savéant, J.-M. *J. Electroanal. Chem.* **2006**, *588*, 197–206. Costentin, C. *Chem. Rev.* **2009**, *108*, 2145–2179.
(8) Venkataraman, C.; Soudackov, A. V.; Hammes-Schiffer, S. *J. Phys. Chem. C* **2008**, *112*, 12386–12397.
(9) Madhiri, N.; Finklea, H. O. *Langmuir* **2006**, *22*, 10643–10651.
(10) Costentin, C.; Robert, M.; Savéant, J.-M.; Teillout, A.-L. *ChemPhysChem* **2009**, *10*, 191–198.
(11) Soudackov, A.; Hatcher, E.; Hammes-Schiffer, S. *J. Chem. Phys.* **2005**, *122*, 014505.
(12) Frisch, M. J. et al. *Gaussian 03*, revision C.03; Gaussian, Inc.: Pittsburgh, PA: 2003.
(13) Liu, Y. P.; Newton, M. D. *J. Phys. Chem.* **1994**, *98*, 7162–7169.
(14) Webb, S. P.; Hammes-Schiffer, S. *J. Chem. Phys.* **2000**, *113*, 5214–5227.

JA910277P